The high-temperature superionic behaviour of Ag_2S

2002 J. Phys.: Condens. Matter 14 L9

(http://iopscience.iop.org/0953-8984/14/1/102)

INSTITUTE OF PHYSICS PUBLISHING JOURNAL OF PHYSICS: CONDENSED MATTER

J. Phys.: Condens. Matter **14** (2002) L9–L17 PII: S0953-8984(02)30211-X

LETTER TO THE EDITOR

The high-temperature superionic behaviour of Ag_2S

S Hull[1], D A Keen[1], D S Sivia[1], P A Madden[2] and M Wilson[3]

[1] The ISIS Facility, Rutherford Appleton Laboratory, Chilton, Didcot, Oxfordshire OX11 0QX, UK
[2] Physical and Theoretical Chemistry Laboratory, Oxford University, South Parks Road, Oxford OX1 3QZ, UK
[3] Department of Chemistry, University College London, Christopher Ingold Laboratories, 20 Gordon Street, London, WC1H 0AJ, UK

Received 30 October 2001, in final form 23 November 2001
Published 7 December 2001
Online at stacks.iop.org/JPhysCM/14/L9

Abstract

Powder neutron diffraction and molecular dynamics (MD) simulations have been used to investigate the structural behaviour of silver sulfide, Ag_2S, at elevated temperatures. Above ∼450 K Ag_2S adopts the β phase in which the S^{2-} possess a body-centred cubic arrangement. Analysis of the neutron diffraction is in good agreement with the previously proposed structural model in which the Ag^+ predominantly reside within the tetrahedral interstices. At ∼865 K Ag_2S transforms to the α phase in which the anion sublattice adopts a face-centred cubic arrangement. Structural refinements of this phase indicate that the cations are distributed predominantly in the tetrahedral cavities but with a significant fraction in the octahedral holes. MD simulations, using established potentials for this compound, confirm the stability of the two high-temperature superionic phases and show good agreement with the measured Ag^+ distribution within the unit cell.

Silver sulfide, Ag_2S, is an important member of the mixed conducting silver and copper chalcogenides, possessing a very high ionic conductivity within its β phase ($\sigma \sim 5\ \Omega^{-1}\ cm^{-1}$ [1]) as well as significant electronic conduction. At room temperature γ-Ag_2S (acanthite) forms a superstructure based on a distorted body-centred cubic (bcc) array of anions with the cations located in sites close to the centres of the tetrahedral and octahedral interstices within the anion sublattice [2]. At 450 K Ag_2S transforms to an α-AgI-like bcc structure (space group $Im\bar{3}m$) with anions in 2(a) (0, 0, 0) sites and the cations spread diffusely in ⟨100⟩ directions between tetrahedral 12(d) and octahedral 6(b) sites, although above ∼473 K the single-crystal neutron diffraction results are best described by occupation of tetrahedral sites only, though with large anharmonic modifications to the thermal parameters [3, 4]. It is reported that at 865 K this bcc phase transforms to a face-centred cubic (fcc) phase. However, this structural assignment is based on rather limited x-ray diffraction data comprising only

one [5] or three [6] reflections and no information concerning the preferred cation locations has been reported.

When considering the systematics of the phase transitions of related materials, the proposed fcc structure for the highest-temperature phase of Ag_2S appears anomalous. Ag_2Te transforms from monoclinic $\rightarrow$ fcc $\rightarrow$ bcc with increasing temperature [7, 8] and AgI transforms from the fcc (zincblende) or hcp(wurtzite) $\rightarrow$ bcc [9, 10], as do CuBr [11, 12], CuI [13] and CuCl [14] (the last two transformations occurring at high temperatures and pressures). Hence, the disordered fcc structure (or related hcp structure) is always the lower-temperature structural modification, with the bcc α-AgI-like structure occurring at higher temperature. In view of the unusual nature of this proposed sequence of phase transitions within Ag_2S and the very limited data from which it has been assigned, an investigation of the structure of the highest-temperature phase of Ag_2S has been performed and is reported here. The ambient-temperature monoclinic phase is labelled γ, the bcc phase β and the highest-temperature phase α.

Neutron diffraction experiments were performed using commercially available Ag_2S powder of stated purity 99.999% provided by Johnson Matthey plc. This was sealed under vacuum inside a $\sim$15 mm diameter silica ampoule of wall thickness $\sim$0.5 mm. The diffraction experiments were performed on the Polaris powder diffractometer at the ISIS facility, UK [15]. Counting times of $\sim$12 h were necessary for each phase, in order to collect data of adequate statistical quality to investigate the preferred Ag^+ locations. The data were corrected for the effects of absorption of the neutron beam by the sample using standard procedures [15] and Rietveld profile refinements using the normalized diffraction data were performed using the program TF12LS [16], which is based on the Cambridge Crystallographic Subroutine Library [17]. The relative quality of fits to the experimental data using different structural models used the usual χ^2 statistic [8, 18].

In addition, the intensities of the Bragg peaks in the powder neutron diffraction data were used to generate maximum entropy (MaxEnt) reconstructions of the time-averaged ionic density within the unit cell. For this analysis, the S^{2-} positions (bcc or fcc) are taken as known and the distribution of Ag^+ is determined. This Bayesian analogue of the difference Fourier method has the advantage that both the phase and amplitude information contained in the 'known fragment' is included. Furthermore, 'physical sense' in the form of local smoothness of the density and its overall positivity can be incorporated in a statistically rigorous manner. Further details of this procedure can be found elsewhere [19].

The structure of the bcc phase, β-Ag_2S, has been investigated previously using neutron and x-ray diffraction methods [3, 4]. The neutron diffraction data collected for β-Ag_2S at $T = 558(2)$ K in this work were fitted using the structural model proposed previously, with the S^{2-} located in the $2(a)$ sites of space group $Im\bar{3}m$ at 0, 0, 0 and $1/2, 1/2, 1/2$ and the $4 \times Ag^+$ per unit cell distributed over the $12(d)$ tetrahedral sites at $1/4$, 0, $1/2$ etc. The results of this procedure are summarized in table 1 and the quality of the least-squares fit is illustrated in figure 1. Attempts to fit other structural models with the Ag^+ distributed over other sites (i.e. $6(b)$ octahedral sites at $1/2, 1/2, 0$ etc; $24(h)$ trigonal sites at $x, x, 0$ etc with $x \sim 3/8$) gave poorer fits to the data. The preference for tetrahedral co-ordination is illustrated in the MaxEnt reconstruction of the scattering (ionic) density within the unit cell (figure 2), though the elongation of the Ag^+ distribution in the $\langle 001 \rangle$ directions suggests that these are the principal conduction pathways.

The principal subject of this work is the α phase observed at temperatures above $\sim$865 K [5, 6, 20]. Using the data collected at $T = 929(2)$ K there are a total of six observable peaks at d-spacings of 3.62, 3.14, 2.22, 1.89, 1.81 and 1.57 Å. These can be identified as the 111, 002, 220, 113, 222 and 004 reflections of an fcc lattice with $a \sim 6.27$ Å. To determine

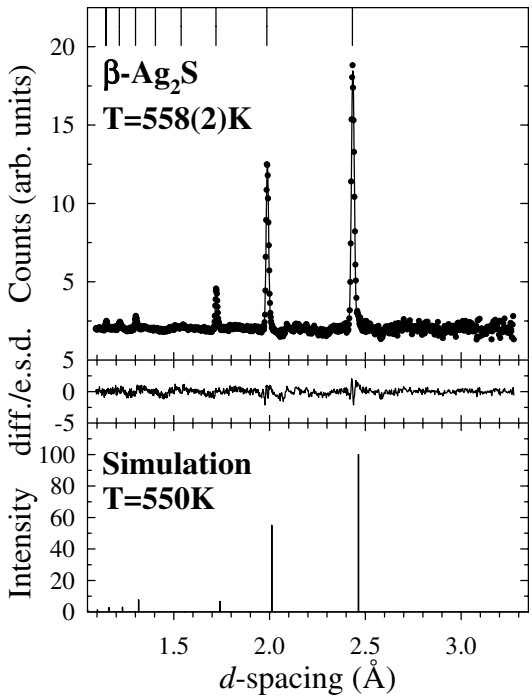

Figure 1. The final least-squares fit to the powder neutron diffraction data collected from β-Ag_2S at $T = 558(2)$ K. The dots are the experimental data points and the solid curve is the calculated profile using the parameters listed in table 1. The middle trace shows the difference (measured minus calculated) divided by the estimated standard deviation on the experimental data points. The tick marks along the top of the figure denote the calculated positions of all the Bragg reflections allowed in $Im\bar{3}m$ symmetry. The lower trace shows the calculated intensities based on the mean ionic distribution determined during the MD simulations at 550 K.

Table 1. Summary of the results of the least-squares fit to the diffraction data collected from β-Ag_2S at $T = 558(2)$ K.

Space group	$Im\bar{3}m$
Lattice parameter	$a = 4.8824(1)$ Å
S^{2-} in 2(a) at 0, 0, 0 etc	
Isotropic thermal parameter	$B_{iso} = 18.5(3)$ Å^2
Ag^+ in 12(d) 1/4, 0, 1/2	
Isotropic thermal parameter	$B_{iso} = 8.9(1)$ Å^2
Goodness-of-fit	$\chi^2 = 1.22$

the correct structure of α-Ag_2S we assume that the anions form an fcc sublattice and consider the possible ways in which the Ag^+ can be distributed over the available interstices. However, since only a limited number of Bragg peaks are observed, caution must be taken to avoid using structural models which introduce more than a few structural variables.

The results are summarized in table 2. The four anions per fcc unit cell are placed in the 4(a) 0, 0, 0 etc sites of space group $Fm\bar{3}m$ and form four octahedral sites (4(b) at 1/2, 1/2, 1/2 etc) and eight tetrahedral sites (8(c) at 1/4, 1/4, 1/4 etc) per unit cell. As a result, there are insufficient octahedral holes available to accommodate all the cations. The first structural

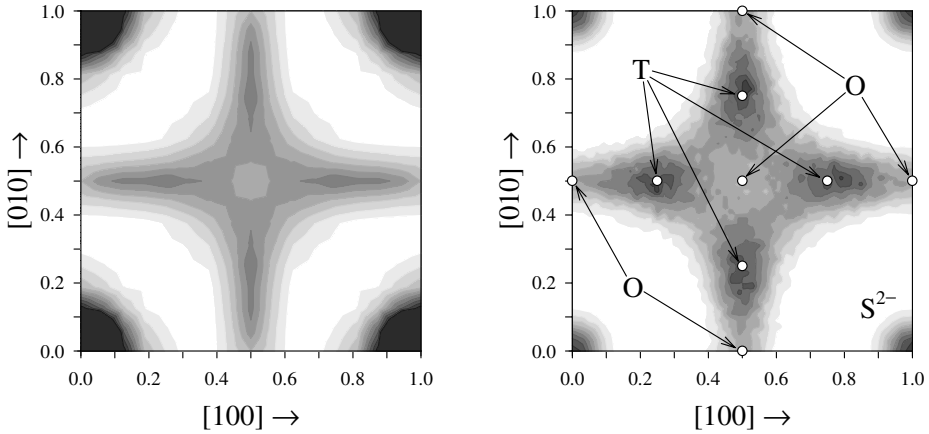

Figure 2. A (001) section at $-0.05 \leqslant z \leqslant 0.05$ showing (left) the experimentally determined ($T = 558(2)$ K) and (right) simulated ($T = 550$ K) mean distribution of ions within an average bcc unit cell of β-Ag_2S. The S^{2-} positions are shown and the octahedral (O) and tetrahedral (T) interstices for the Ag^+ are indicated.

model (model A) places the cations on all the tetrahedral positions, but this provides a relatively poor fit to the data. Model B allows the occupation of the tetrahedral sites to vary, though without constraining the displaced cations to occupy specific crystallographic sites. Though physically unrealistic, the final value of occupancy of the tetrahedral sites (∼5) suggests that significant numbers of cations are displaced from these sites. Model C attempts to mimic the effects of anharmonic cation thermal vibrations by 'splitting' each of the tetrahedral sites into partially filled sites which are displaced a short distance (∼0.5 Å) in the ⟨111⟩ directions away from the cations. Model D distributes the cations equally over the octahedral and tetrahedral positions, such that the former are completely filled. As shown by the value of χ^2 in table 2, this produces a significant improvement in the quality of the fit. Allowing the distribution of Ag^+ to vary over the two sites (model E) produces a further slight improvement in χ^2, with a tendency towards a preferred occupancy of the tetrahedral positions. Models F and G are extensions of model E and displace those cations on the octahedral sites in ⟨110⟩ and ⟨111⟩ directions, respectively. The latter gives a slight improvement in χ^2 but, in view of the limited number of measured peaks, this cannot be considered significant and we conclude that model E gives the best structural description of α-Ag_2S. The quality of the fit is illustrated in figure 3. The time-averaged distribution of Ag^+ is further demonstrated by the MaxEnt reconstruction of the scattering (ionic) density, as illustrated for the case of a $(1\bar{1}0)$ section through the unit cell in figure 4.

The molecular dynamics (MD) used the so-called RVP potential, which has been widely used to simulate the ionic diffusion processes in various phases of Ag^+- and Cu^+-based compounds [21–28]. The potential between ions i and j has the general form

$$V_{ij}(r) = \frac{H_{ij}}{r^{n_{ij}}} + \frac{Z_i Z_j e^2}{r} - \frac{1}{2}\left(\alpha_i Z_j^2 + \alpha_j Z_i^2\right)\frac{e^2}{r^4} - \frac{W_{ij}}{r^6},$$

where $H_{ij} = A_{ij}(\sigma_i + \sigma_j)^{n_{ij}}$, A_{ij} is the short-range repulsive strength and σ_i and σ_j are the ionic radii. The ionic charges Z_i and Z_j are typically lower than their formal (ionic) values. α_i and α_j are the electronic polarizibilities and W_{ij} are the coefficients of the Van der Waals interaction.

For the case of Ag_2S, values of the parameters in the above expression have been

Table 2. The values of the goodness-of-fit parameter χ^2 obtained by least-squares fitting of the diffraction data collected from α-Ag_2S at $T = 929(2)$ K using the structural models A to G. $a = 6.2698(3)$ Å, space group $Fm\bar{3}m$, S^{2-} in 4(a) at 0, 0, 0 etc.

				S	Ag1			Ag2		
	Model		χ^2	B (Å^2)	B (Å^2)	x	n	B (Å^2)	x	n
A	Ag1 in 8(c) 1/4, 1/4, 1/4	Tetrahedral sites only	1.89	14.2(6)	25.4(8)		8			
B	Ag1 in 8(c) 1/4, 1/4, 1/4	Partial occ. of tet.	1.77	18.7(7)	16.9(9)		5.0(2)			
C	Ag2 in 32(f) x, x, x	Displaced tetrahedral	1.53	14.0(6)	9.4(8)	0.308(1)	8			
D	Ag1 in 8(c) 1/4, 1/4, 1/4	Tetrahedral and	1.21	14.7(7)	17.4(8)		4	$=B_{Ag1}$		4
	Ag2 in 4(b) 1/2, 1/2, 1/2	Octahedral sites								
E	Ag1 in 8(c) 1/4, 1/4, 1/4	As model D but	1.10	13.5(6)	31(1)		5.3(1)	40(3)		2.7(1)
	Ag2 in 4(b) 1/2, 1/2, 1/2	variable occupancy								
F	Ag1 in 8(c) 1/4, 1/4, 1/4	Tetrahedral + ⟨110⟩	1.12	13.0(7)	35(2)		5.9(1)	36(7)	0.382(1)	2.1(1)
	Ag2 in 48(i) x, x, 1/2	displaced oct.								
G	Ag1 in 8(c) 1/4, 1/4, 1/4	Tetrahedral + ⟨111⟩	1.08	14.0(8)	22(1)		3.9(1)	25(2)	0.392(1)	4.1(1)
	Ag2 in 32(f) x, x, x	displaced oct.								

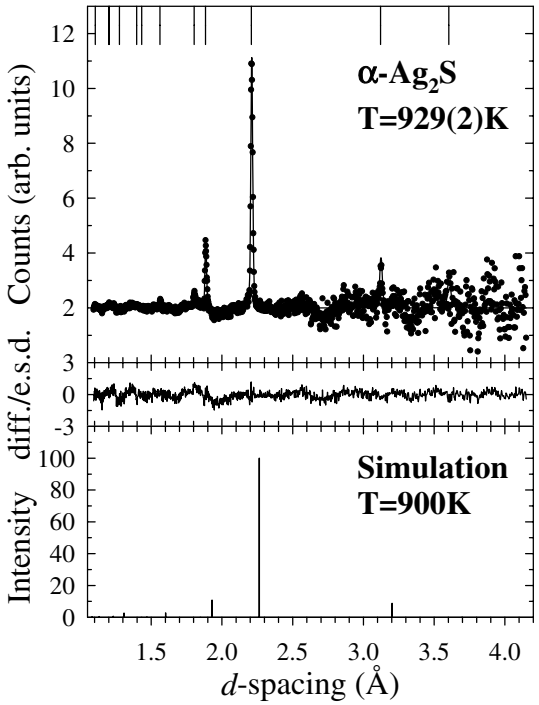

Figure 3. The final least-squares fit to the powder neutron diffraction data collected from α-Ag_2S at $T = 929(2)$ K. The dots are the experimental data points and the solid curve is the calculated profile using the parameters listed in table 2. The middle trace shows the difference (measured minus calculated) divided by the estimated standard deviation on the experimental data points. The tick marks along the top of the figure denote the calculated positions of all the Bragg reflections allowed in $Fm\bar{3}m$ symmetry. The lower trace shows the calculated intensities based on the mean ionic distribution determined during the MD simulations.

determined previously [24, 25], with the simplifying assumptions that $A_{ij} = A = 0.015\,02$, $n_{ij} = n = 7$ and neglect of the last term (i.e. $W_{ij} = 0$). The other values are $Z_{Ag+} = 0.45$ and $Z_{S^{2-}} = -0.9$, $\sigma_{Ag+} = 0.61$ Å and $\sigma_{S^{2-}} = 2.1$ Å, $\alpha_{Ag+} = 0$ and $\alpha_{S^{2-}} = 6.52$ Å^3. Simulations were performed at constant (zero) pressure and at temperatures of 550 and 900 K, these being chosen as close to the temperatures at which the two phases were measured in the neutron diffraction studies and close to the experimentally observed $\beta \rightarrow \alpha$ transition temperature (865 K) [20]. The systems contained a total of $N_a = 750$ ions (β-Ag_2S) and $N_a = 768$ ions (α-Ag_2S). Periodic boundary conditions were applied. The simulations were allowed to equilibrate for ~60 ps and then a subsequent run of ~60 ps was used for analysis of the ionic motions. The mean distribution of ions within the unit cell was determined by averaging over time t and over all the unit cells in the simulation box. This was then used to determine a simulated Bragg diffraction pattern for comparison with the experimental data.

The MD simulations of the β phase of Ag_2S were also found to be in good agreement with those presented previously [24]. This is to be expected, since the same interionic potential is used, though a fixed simulation box volume was used in the earlier work. As illustrated in figure 5, the mean squared displacements of the Ag^+ and S^{2-} within the β phase show rapid motion of the cations and no evidence of diffusion of the anions. This is indicative of a stable superionic phase. Of particular interest in this work is the distribution of Ag^+ within the unit

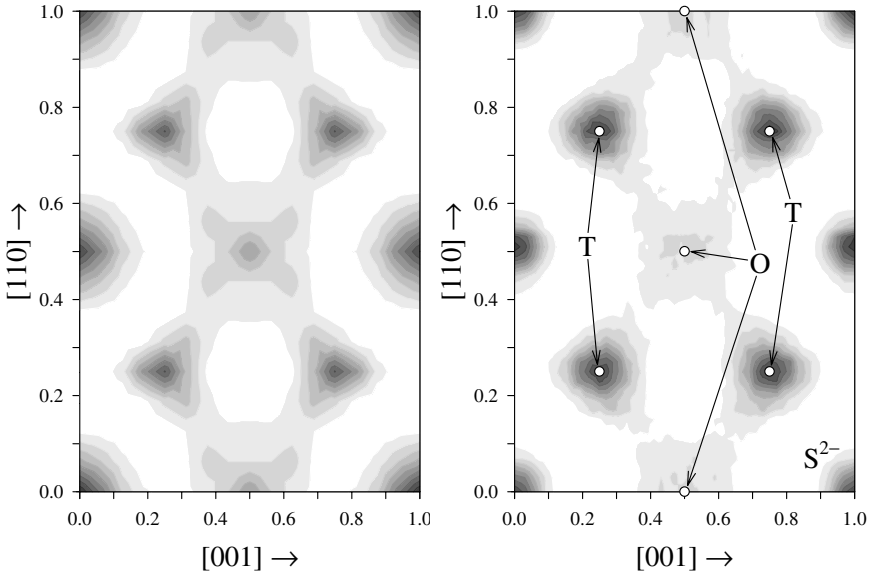

Figure 4. A $(1\bar{1}0)$ section $-0.05 \leqslant z \leqslant 0.05$ showing (left) the experimentally determined ($T = 929(2)$ K) and (right) simulated ($T = 900$ K) mean distribution of ions within an average fcc unit cell of α-Ag_2S. The S^{2-} positions are shown and the octahedral (O) and tetrahedral (T) interstices for the Ag^+ are indicated.

cell, which is illustrated for the case of a (001) section in figure 2. This clearly shows the preferential occupancy of the tetrahedral positions (labelled T). However, the density extends between the tetrahedral sites in [001] directions and suggests that the Ag^+ conduction occurs via the octahedral sites. However, the absence of a peak in the density at these positions indicate that the Ag^+ do not reside in these positions. This supports the neutron diffraction analysis described above, where attempts to include the octahedral sites were unsuccessful. The calculated diffraction intensities based on the time-averaged structure derived from the MD simulations (shown at the bottom of figure 1) are in excellent agreement with those measured.

The previous MD studies of Ag_2S [24, 25] considered only the bcc-structured β phase and we now investigate whether the same potential can be used to stabilize the fcc-structured arrangement found in α-Ag_2S. These simulations started from an ordered arrangement with all the Ag^+ placed in the ideal tetrahedral sites (i.e. the antifluorite-structured model A discussed above). However, after $\sim$10 ps, a dynamic equilibrium configuration was obtained in which the Ag^+ undergo rapid diffusion (see figure 5) and, as shown in figure 4, a significant fraction of the Ag^+ are displaced onto the octahedral positions.

The agreement between the MD simulations and the powder neutron diffraction results is slightly less impressive for α-Ag_2S than β-Ag_2S. Whilst the calculated Bragg intensities using the simulated ionic distribution (bottom of figure 3) are in relatively good agreement, the ratio of octahedral to tetrahedral occupation in the simulations is around 1:4 rather than the close to 1:2 distribution obtained by the experimental method. Nevertheless, there is clear evidence in figure 4 that the octahedral positions are stable sites for the Ag^+ within the fcc S^{2-} sublattice and, therefore, the conduction pathways are between tetrahedral sites via the octahedral positions.

The work presented in this Letter clearly shows that Ag_2S transforms from bcc to fcc on increasing temperature at $T = 860(10)$ K, in contrast to Ag_2Te, which transforms from fcc

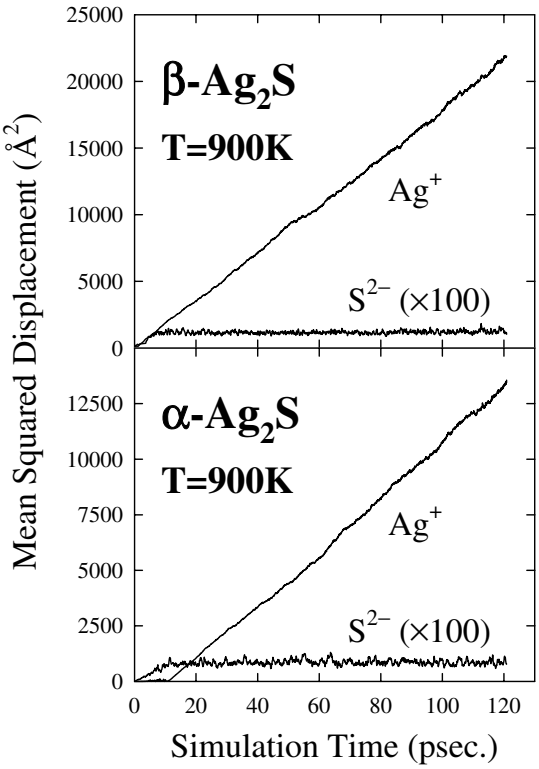

Figure 5. The mean squared displacements of Ag^+ and S^{2-} ions in the MD simulations of β-Ag_2S (top) and α-Ag_2S (bottom) at 900 K.

to bcc at $T \sim 1075$ K [7, 8]. As such, they provide the possibility for assessing the relative merits of fcc and bcc anion sublattices in promoting superionic behaviour. Measurements of the ionic conductivity show that the bcc-structured phase has a higher ionic conductivity than the fcc-structured phase in both Ag_2S and Ag_2Te [1]. This is supported by the slopes of the mean squared displacement versus time plots (figure 5), which, as $t \rightarrow \infty$, are proportional to the Ag^+ diffusion coefficient, D_{Ag+}. However, it is necessary to determine the relative densities of the two phases and detailed measurements of the thermal expansion of both Ag_2S and Ag_2Te (including the volume discontinuities at the structural transitions) using powder neutron diffraction are planned. It is interesting to note that the MD simulations of Ag_2S predict that the unit cell volume per formula unit of the bcc phase is $\sim$3.9 and $\sim$2.3% lower than the fcc one at 550 and 900 K, respectively. If confirmed experimentally, this implies that β-Ag_2S has a higher ionic conductivity than α-Ag_2S, despite having a higher density. This is probably a consequence of the preferred tetrahedral co-ordination of the Ag^+ and the specific geometric properties of the bcc sublattice, which allows all the cations to be accommodated within a network of many interconnected tetrahedral sites. Similar arguments have been proposed to explain the higher ionic conduction of bcc-structured phases of the Ag^+ and Cu^+ monohalides in comparison with the fcc-structured ones [29].

The work presented in this Letter forms part of a wider research project investigating the structural and dynamical behaviour of superionic conductors funded by the Engineering and Physical Sciences Research Council (reference GR/M38711). We are grateful to I Ebbsjö

for advice concerning the RVP potential and to J Dreyer for assistance with the sample encapsulation and operation of the neutron furnace.

References

[1] Miyatani S 1981 *J. Phys. Soc. Japan* **50** 3415
[2] Sadanaga R and Sueno S 1967 *Miner. J. (Japan)* **5** 124
[3] Cava R J and McWhan D B 1980 *Phys. Rev. Lett.* **45** 2046
[4] Cava R J, Reidinger F and Wuensch B J 1980 *J. Solid State Chem.* **31** 69
[5] Djurle S 1958 *Acta Chem. Scand.* **12** 1427
[6] Frueh A J 1961 *Am. Mineral.* **46** 654
[7] Schneider J and Schulz H 1993 *Z. Kristallogr.* **203** 1
[8] Keen D A and Hull S 1998 *J. Phys.: Condens. Matter* **10** 8217
[9] Wright A F and Fender B E F 1977 *J. Phys. C: Solid State Phys.* **10** 2261
[10] Nield V M, Keen D A, Hayes W and McGreevy R L 1993 *Solid State Ion.* **66** 247
[11] Bührer W and Hälg W 1977 *Electrochim. Acta* **22** 701
[12] Nield V M, McGreevy R L, Keen D A and Hayes W 1994 *Physica* B **202** 159
[13] Hull S, Keen D A, Hayes W and Gardner N J G 1998 *J. Phys.: Condens. Matter* **10** 10 941
[14] Hull S and Keen D A 1996 *J. Phys.: Condens. Matter* **8** 6191
[15] Hull S, Smith R I, David W I F, Hannon A C, Mayers J and Cywinski R 1992 *Physica* B **180/181** 1000
[16] David W I F, Ibberson R M and Matthewman J C 1992 *Rutherford Appleton Laboratory Report* RAL-92-032
[17] Brown P J and Matthewman J C 1987 *Rutherford Appleton Laboratory Report* RAL-87-010
[18] Wilson A J C (ed) 1995 *International Tables for Crystallography* vol C (Dordrecht: Kluwer)
[19] Sivia D S and David W I F 2001 *J. Phys. Chem. Solids* **62** 2119–27
[20] Grønvold F and Westrum E F 1986 *J. Chem. Thermodyn.* **18** 381
[21] Vashishta P and Rahman A 1978 *Phys. Rev. Lett.* **40** 1337
[22] Parrinelo M, Rahman A and Vashishta P 1983 *Phys. Rev. Lett.* **50** 1073
[23] O'Sullivan K, Chiarotti G and Madden P A 1991 *Phys. Rev.* B **43** 13 536
[24] Vashishta P, Ebbsjö I, Dejus R and Sköld K 1985 *J. Phys. C: Solid State Phys.* **18** L291
[25] Ebbsjö I, Vashishta P, Dejus R and Sköld K 1987 *J. Phys. C: Solid State Phys.* **20** L441
[26] McGreevy R L and Zheng-Johansson J X M 1997 *Solid State Ion.* **95** 215
[27] Ihata K and Okazaki H 1997 *J. Phys.: Condens. Matter* **9** 1477
[28] Madden P A, O'Sullivan K F and Chiarotti G 1992 *Phys. Rev.* B **45** 10 206
[29] Boyce J B and Huberman B A 1979 *Phys. Rep.* **51** 189